Molecular Therapy
Nucleic Acids
Original Article

Permanent Inactivation of HBV Genomes by CRISPR/Cas9-Mediated Non-cleavage Base Editing

Yu-Chan Yang,[1] Yu-Hsiang Chen,[1] Jia-Horng Kao,[2,3,4,5] Chi Ching,[1] I-Jung Liu,[6] Chih-Chiang Wang,[2] Cheng-Hsueh Tsai,[2] Fang-Yi Wu,[1] Chun-Jen Liu,[2,3,4,5] Pei-Jer Chen,[2,3,4,5] Ding-Shinn Chen,[2,3,4,5] and Hung-Chih Yang[1,2,3]

[1]Department of Microbiology, National Taiwan University College of Medicine, National Taiwan University Hospital, Taipei, Taiwan; [2]Graduate Institute of Clinical Medicine, National Taiwan University College of Medicine, National Taiwan University Hospital, Taipei, Taiwan; [3]Department of Internal Medicine, National Taiwan University College of Medicine, National Taiwan University Hospital, Taipei, Taiwan; [4]Hepatitis Research Center, National Taiwan University College of Medicine, National Taiwan University Hospital, Taipei, Taiwan; [5]Department of Medical Research, National Taiwan University College of Medicine, National Taiwan University Hospital, Taipei, Taiwan; [6]Department of Nursing, Cardinal Tien Junior College of Healthcare and Management, New Taipei City, Taiwan

Current antiviral therapy fails to cure chronic hepatitis B virus (HBV) infection because of persistent covalently closed circular DNA (cccDNA). CRISPR/Cas9-mediated specific cleavage of cccDNA is a potentially curative strategy for chronic hepatitis B (CHB). However, the CRISPR/Cas system inevitably targets integrated HBV DNA and induces double-strand breaks (DSBs) of host genome, bearing the risk of genomic rearrangement and damage. Herein, we examined the utility of recently developed CRISPR/Cas-mediated "base editors" (BEs) in inactivating HBV gene expression without cleavage of DNA. Candidate target sites of the SpCas9-derived BE and its variants in HBV genomes were screened for generating nonsense mutations of viral genes with individual guide RNAs (gRNAs). SpCas9-BE with certain gRNAs effectively base-edited polymerase and surface genes and reduced HBV gene expression in cells harboring integrated HBV genomes, but induced very few insertions or deletions (indels). Interestingly, some point mutations introduced by base editing resulted in simultaneous suppression of both polymerase and surface genes. Finally, the episomal cccDNA was successfully edited by SpCas9-BE for suppression of viral gene expression in an *in vitro* HBV infection system. In conclusion, Cas9-mediated base editing is a potential strategy to cure CHB by permanent inactivation of integrated HBV DNA and cccDNA without DSBs of the host genome.

INTRODUCTION

Chronic hepatitis B virus (HBV) infection often leads to adverse clinical outcomes, including cirrhosis and hepatocellular carcinoma (HCC).[1] Although current antiviral therapies have dramatically improved the outcomes of individuals with chronic hepatitis B (CHB), most patients experience rebound viremia after discontinuation of nucleos(t)ide analogs (NAs).[2] The major obstacle for eradicating HBV infection by NAs is the persistent covalently closed circular DNA (cccDNA), which is the episomal form of a virally replicative template.[3] Curative strategies for CHB need to either eliminate all of the infected hepatocytes or purge all of the replication-competent cccDNA.[4,5] So far, curing HBV remains extremely challenging because no drugs can specifically target and destroy cccDNA.

Integration of HBV DNA into host genomes is a common event occurring upon HBV infection.[6,7] Unlike retrovirus, HBV integration is not a requisite for the viral life cycle because integrated HBV DNA does not serve as a template for productive viral replication.[8] Nevertheless, integrated HBV DNA has recently been proven to be a crucial source for the continuous secretion of hepatitis B surface antigen (HBsAg).[9] An excessive amount of secreted HBsAg likely has the immunosuppressive effect and acts as a "decoy" for antibody responses in order to allow HBV to escape from host immunological control.[10] Recently, there has been emerging enthusiasm for the functional cure of HBV, which is defined as loss of HBsAg. However, disruption of cccDNA alone may not necessarily result in HBsAg loss. It is reasonably assumed that a functional HBV cure cannot be achieved without targeting integrated HBV genomes.[11]

The recent advance of genome-editing tools has provided a novel approach to treat viral infections by cutting and destroying viral genomes in a sequence-specific manner.[12–15] Particularly, the CRISPR/Cas RNA-guided DNA endonuclease has gained the widest interest because it can be conveniently redirected to the desired DNA sequences by simply redesigning the sequences of guide RNAs (gRNAs) that are perfectly matched with the protospacer sequences

https://doi.org/10.1016/j.omtn.2020.03.005.

Correspondence: Hung-Chih Yang, MD, PhD, Department of Microbiology, National Taiwan University College of Medicine, National Taiwan University Hospital, Basic Medical Sciences Building, Room 724, 1, Jen-Ai Road, Section 1, Taipei 10051, Taiwan.
E-mail: hcyang88@ntu.edu.tw

of the target genomes. Cleavage of target genomes by Cas9/gRNA causes double-strand breaks (DSBs) of DNA, which are often repaired by the non-homologous end joining (NHEJ) pathway.[16,17] The NHEJ pathway frequently leads to nucleotide insertions or deletions (indels) and thus disrupts the open reading frames (ORFs) of genes.

Previous studies, including ours, have examined the utility of CRISPR/Cas9 in disruption of HBV genomes.[18–22] Most studies have taken advantage of the wild-type (WT) CRISPR/Cas9 system and demonstrated its utility in specific cleavage of intrahepatic HBV templates, including cccDNA and integrated HBV genomes, for curing HBV infection.[23,24] However, the CRISPR-meditated cleavage of integrated HBV DNA also results in DSBs of the host genome, which may cause large deletions and chromosomal rearrangements, leading to pathological consequences.[25] Recently, a novel CRISPR-derived base-editing strategy has been shown to generate precise C-T/G-A conversion without DSBs at specific genome loci.[26] The initial "base editors" (BEs) utilized a catalytically impaired Cas9 endonuclease (dCas9) tethered with APOBEC deaminase. To enhance C-T/G-A conversion, the dCas9-deaminase construct was fused with a uracil glycosylase inhibitor (UGI) that suppresses uracil excision following deamination to prevent the reversion of the U:G pair to a C:G pair. A widely used third-generation BE (BE3) was thus designed with the combination of APOBEC1, Cas9-derived nickase, and UGI.[27] Since then, a growing number of modified BEs have been developed to improve various aspects of BE tools.[28] For example, the fourth-generation BE4 increases the efficiency of C-T/G-A conversion, while halving the frequency of undesired base changes compared to BE3. BE4Gam is generated by fusing BE4 to DSB-binding protein Gam from bacteriophage Mu to further reduce indel formation.[29] In addition, the efficacy of base editing can be significantly improved by optimizing codon usage (BE^{RA}), and further enhanced by including nuclear targeting motifs at the N terminus of BE enzymes (FNLS-BEs).[30] Theoretically, base editing the target nucleotides without DSBs of DNA should reduce the risk of genome rearrangement and carcinogenesis.[26] Although interesting, the effect of the Cas9-mediated BE on the episomal cccDNA remains unclear.

In this study, we explored the utility and efficacy of the CRISPR/Cas9-derived BEs in introducing nonsense mutations to cccDNAs and integrated HBV genomes. We screened the entire HBV genomes and identified candidate sites that could effectively be base edited to create premature stop codons of viral genes. We further proved the successful base editing of integrated HBV DNAs and cccDNAs and the reduced expression of both surface and polymerase genes, demonstrating the potential for curing HBV by Cas9-BE.

RESULTS

Designing and Screening HBV-Specific gRNAs for Inducing Nonsense Mutations by SpCas9 BEs

To construct the HBV-specific gRNAs that are suitable for an SpCas9 base editor (SpCas9-BE), we first searched for the candidate protospacer sequences across the four ORFs of the HBV genome by using the website software BE-Designer.[8] We identified 23 candidate target sequences, including 3 in the core, 9 in polymerase, 9 in the surface, and 2 in X ORFs (Figure 1A; Table 1). HBV-specific gRNAs were then constructed and co-transfected with codon-optimized FNLS-P2A-Puro (puromycin), hereafter named BE3 for the sake of simplicity, into integrated HBV genome-containing HEK293T cells (HBV-HEK293T cells), including HEK293T-core, HEK293T-polymerase (pol), and HEK293T-surface cells. The efficiency of C-T/G-A conversion in these gRNA targeting sites was evaluated by Sanger sequencing (Figure 1B). The ratio of C-T/G-A conversion at each target site was roughly categorized as approximately 0%, less than 50%, approximately 50%, and greater than 50%. The information and base-editing efficiency for each gRNA are summarized in Table 1. The extent of sequence conservation for the protospacer sequence and protospacer adjacent motif (PAM) of each gRNA is summarized in Table S1. Overall, among all of the screened HBV-specific gRNAs, we discovered 14 gRNAs targeting the polymerase and surface ORFs with base-editing efficiency of approximately or greater than 50%, whereas the gRNAs targeting the core and X ORFs has less optimal base-editing efficiency (approximately 0% or less than 50%).

We also performed the screening for candidate gRNAs using SpCas9-BE variants, including VQR, VRER, and EQR, which recognize altered PAMs NGAN, NGCG, and NGAG, respectively (Figure S1A).[31] The results are summarized in Figure S1B and Table S2, which show that the overall editing efficiency of SpCas9-BE variants was lower than that of the natural SpCas9-BE.

Inhibition of the Expression of HBsAg and Polymerase by Introducing Nonsense Mutations into Integrated HBV Genomes through Base Editing

As mentioned above, continuous expression of HBsAg from the integrated HBV genomes prevents loss of HBsAg. We thus examined whether the selected gRNAs combined with BE4Gam-P2A-Puro were able to suppress the expression of viral genes from integrated HBV genomes, particularly HBsAg, in HepG2.2.15, which harbors integrated replication-competent dimeric HBV genomes.[32] BE4Gam-P2A-Puro, hereafter named BE4, contains codon-optimized dCas9 nickase and nuclear targeting motifs and Gam at the N terminus, and thus has higher base-editing efficacy and reduced undesired base changes and indel formation compared to BE3.[30] We chose a number of gRNAs targeting surface ORFs with high base-editing efficiency, including gS3 (preS2), gS7 (S), and gS8 (S). Following lentiviral transduction of HepG2.2.15 cells with gRNAs and BE4 twice, the supernatants and lysates of HepG2.2.15 cells were collected to examine the expression of HBsAg by a semiquantitative ELISA and immunoblotting, respectively. The genomic DNA (gDNA) was also extracted for Sanger sequencing. The results show the ratios of successful C-T/G-A conversion at target sites of gS3, gS7, and gS8 were $\geq$50%, $\geq$50%, and approximately 50%, respectively (Figure 2). Additionally, a significant decline of HBsAg secretion was observed in the supernatants of HepG2.2.15 cells treated with gS7 and gS8,

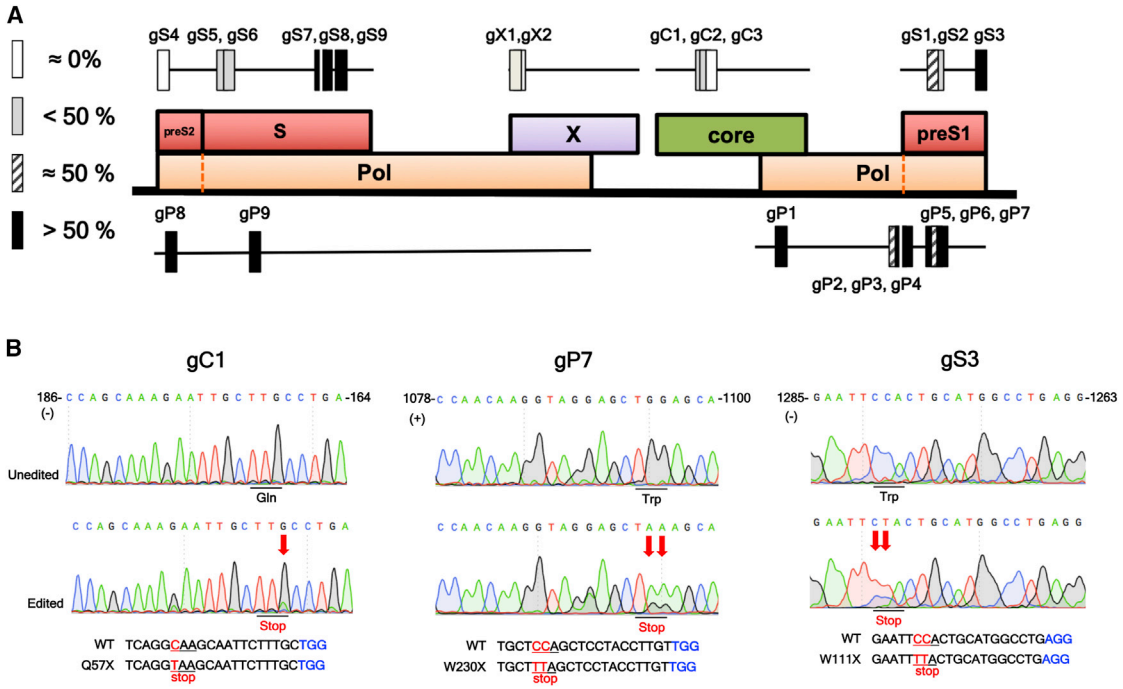

Figure 1. Screening gRNAs for SpCas9-Mediated Base Editing in HBV-HEK293T Cells

(A) Schematic illustration of the HBV genome with four ORFs, including core, polymerase, surface, and X, targeted by the gRNAs/SpCas9 base editors. The small rectangles above or below the HBV genome indicate individual gRNA-targeted sites, with four forms representing the approximate percentages of C-T/G-A conversion, including black (>50%), hatched (approximately 50%), light gray (<50%), and white (approximately 0%). (B) Sanger sequencing of three representative base-edited sites targeted by individual gRNAs, including gC1 (core), gP7 (polymerase), and gS3 (surface) in HBV-HEK293T cells. The upper panel shows the Sanger sequencing results of the control gRNA-treated (unedited) samples and the indicated gRNA-treated (edited) samples. The number and the plus or minus signs at the top indicate the nucleotide position and the DNA sense. The red arrows indicate the edited sites. The sequences at the bottom are the wild-type (top) and base-edited (bottom) protospacer sequences with PAM (blue). The base-edited nucleotides are marked in red, and mutated amino acids are underlined. WT, wild-type.

which target an S gene, whereas cells treated with gS3, which targets a pre-S2 gene, did not show significant HBsAg reduction (Figure 2A). The expression of HBsAg was also confirmed by immunoblotting analysis, which shows a pattern of HBsAg reduction similar to the ELISA results. Only HepG2.2.15 cells treated with gS7 and gS8, but not those treated with gS3, exhibited significantly decreased expression of small surface protein (Figure 2B).

Furthermore, we examined the effect of base-editing inactivation on HBV polymerase by utilizing gRNAs with high efficiency, that is, gP7, gP8, and gP9, which target protospacer sequences that are conserved in 88% of genotype D HBV strains. We generated lentiviruses of gRNAs and BE4 and co-transduced HepG2.2.15 with them twice during an interval of 14 days. gDNA was subsequently extracted from transduced cells and subjected to Sanger sequencing. The results show that the C-T/G-A conversion rates at all three sites are approximately 50% (Figure S2). The HBV DNA level of the supernatants in HepG2.2.15 cells treated with gP7, gP8, and gP9 decreased by more than 60%, indicating effective inactivation of HBV replication (Figure 2C). In addition, the effective base editing was further confirmed by next-generation sequencing (NGS), which showed that the C-T/G-A conversion rates at the target sites of gP7, gP8, gP9, gS3, gS7, and gS8 were around 35%–80% (Figure 2D). To evaluate the specificity of Cas9-BE, we analyzed the off-target effects of base editing for two of the most effective gRNAs (gP9 and gS8). We chose the top three predicted off-target sites for each gRNA. The mutagenesis rates of all of the off-target sites measured by NGS were very low (Figure S3). Finally, we analyzed the frequency of Cas9-BE-induced on-target indels by NGS. Measurement of indels can be used to evaluate the risk of DSB, which is often repaired by the NHEJ mechanism and causes indels. Our results showed that base editing with all of the above six gRNAs (gP7, gP8, gP9, gS3, gS7, and gS8) resulted in low on-target indels (0.5%–5%). We further compared the frequencies of indels caused by WT Cas9 and Cas9-BE at the target sites of gP9, gS7, and gS8 and found that WT Cas9 indeed induced significantly much higher levels of indels (>70%) than did Cas9-BE (Figure 2E).

Dual Suppression of HBsAg and Polymerase by Base Editing-Specific Loci of the HBV Genome

The HBV genome is compactly organized and arranged into four ORFs with substantial overlapping regions. Therefore, we were interested to determine whether the nucleotide change in the ORF of polymerase would introduce a missense mutation and

Table1. Base-Editing Efficiency of SpCas9-BE with Individual gRNAs

Name	Nucleotide Position	ORF	Site of ORF	Strand	Protospacer	Editing %
gC1	164–186	C	Q57	+	TCAGGCAAGCAATTCTTTGC	<50
gC2	165–187	C	Q57	+	CAGGCAAGCAATTCTTTGCT	<50
gC3	166–188	C	Q57	+	AGGCAAGCAATTCTTTGCTG	0
gP1	630–608	P	W74	–	TTCCAATGAGGATTAAAGAC	>50
gP2	929–951	P	Q177	+	TGGGAACAAGATCTACAGCA	≅50
gP3	930–952	P	Q177	+	GGGAACAAGATCTACAGCAT	>50
gP4	931–953	P	Q177	+	GGAACAAGATCTACAGCATG	>50
gP5	1048–1070	P	Q217	+	TCAATCCCAACAAGGACACC	>50
gP6	1074–1096	P	Q225	+	GACGCCAACAAGGTAGGAGC	≅50
gP7	1078–1100	P	W230	–	TGCTCCAGCTCCTACCTTGT	>50
gP8	1350–1328	P	W313/314	–	AGCCACCAGCAGGGAAATAC	>50
gP9	1654–1632	P	W414	–	CGATAACCAGGACAAGTTGG	>50
gS1	1075–1053	pre-S1	W41	–	TCTGGCCAGGTGTCCTTGTT	≅50
gS2	1076–1054	pre-S1	W41	–	GTCTGGCCAGGTGTCCTTGT	<50
gS3	1285–1263	pre-S2	W111	–	GAATTCCACTGCATGGCCTG	>50
gS4	1305–1327	pre-S2	Q121	+	CTGCAAGATCCCAGAGTGAG	0
gS5	1519–1541	S	W193	+	TACCGCAGAGTCTAGACTCG	<50
gS6	1543–1521	S	W198	–	CACCACGAGTCTAGACTCTG	<50
gS7	1909–1887	S	W319	–	AAAGCCCAGGATGATGGGAT	>50
gS8	1910–1888	S	W319	–	GAAAGCCCAGGATGATGGGA	>50
gS9	1955–1933	S	W335	–	GAGCCAGGAGAAACGGGCTG	>50
gX1	2672–2694	X	G8	+	GCTGCCAACTGGATCCTGCG	<50
gX2	2673–2695	X	G8	+	CTGCCAACTGGATCCTGCGC	<50

influence the expression of surface protein and vice versa. Actually, the three gRNAs, gP7, gP8, and gP9, not only generated nonsense mutations in the polymerase gene, but they also resulted in G50L (pre-S1), G25/26N (pre-S2), and G71N (S) missense mutations in the surface ORFs. We found that the HBsAg levels of the supernatants from HepG2.2.15 treated by gP8 and gP9 decreased significantly using a semiquantitative HBsAg ELISA assay (Figure 3A). The decline of HBsAg was even more profound in gP9-treated cells. In contrast, there was no significant decrease of HBsAg level in the supernatant of gP7-treated cells. Consistently, immunoblotting analysis of cell lysates also showed a similar pattern of the reduced surface antigen expression (Figure 3B). Likewise, the three gRNAs, gS3, gS7, and gS8, not only caused nonsense mutations in the surface gene, but also led to E292L (gS3) and G500S (gS7 and S8) missense mutations in the polymerase gene. Interestingly, the HBV DNA levels in the supernatants of HepG2.2.15 cells treated with gS3, gS7, and gS8 also decreased significantly (Figure 3C). Taken together, we demonstrate that the expression of both polymerase and surface genes can be significantly reduced by simultaneous introduction of a missense mutation into the polymerase gene and a nonsense mutation into the surface gene, respectively, or vice versa using gRNAs targeting the overlapping regions of these two genes.

Validation of the Dual Suppression Phenomenon by Specific Point Mutations of the HBV Genome

To further confirm the effective dual suppression of polymerase and surface gene expression by the particular gRNAs, including gP9, gS7, and gS8, we intentionally introduced these nonsense mutations into HBV genomes by site-directed mutagenesis, including W156X in the surface (W156X-S) and W414X in polymerase (W414X-P), which correspond with the base-editing sites of gS7/gS8 (same base-editing site) and gP9 (Figure 4A). Because the surface and polymerase genes of the HBV genome are extensively overlapped, the W156X-S nonsense mutation also introduces G500S in polymerase, and W414X-P causes G71N in the S gene as well. By transfection of Huh7 cells with the WT or mutant HBV-expression plasmid, we observed that the W156X-S nonsense mutation led to dramatic HBsAg reduction in the supernatant and cytoplasm to below the detection limit, and the G71N missense mutation (W414X-P) also caused a significant decrease of HBsAg (Figures 4B and 4C). In addition, for the mutations in the polymerase gene, both the W414X-P nonsense mutation and the G500S missense mutation (W156X-S) resulted in significant reduction of the viral DNA in the supernatant at 5 days post-transfection (Figure 4D). We further performed a Southern blot to measure the intracellular replicative intermediates of transfected cells and found that the two mutant HBV genomes with

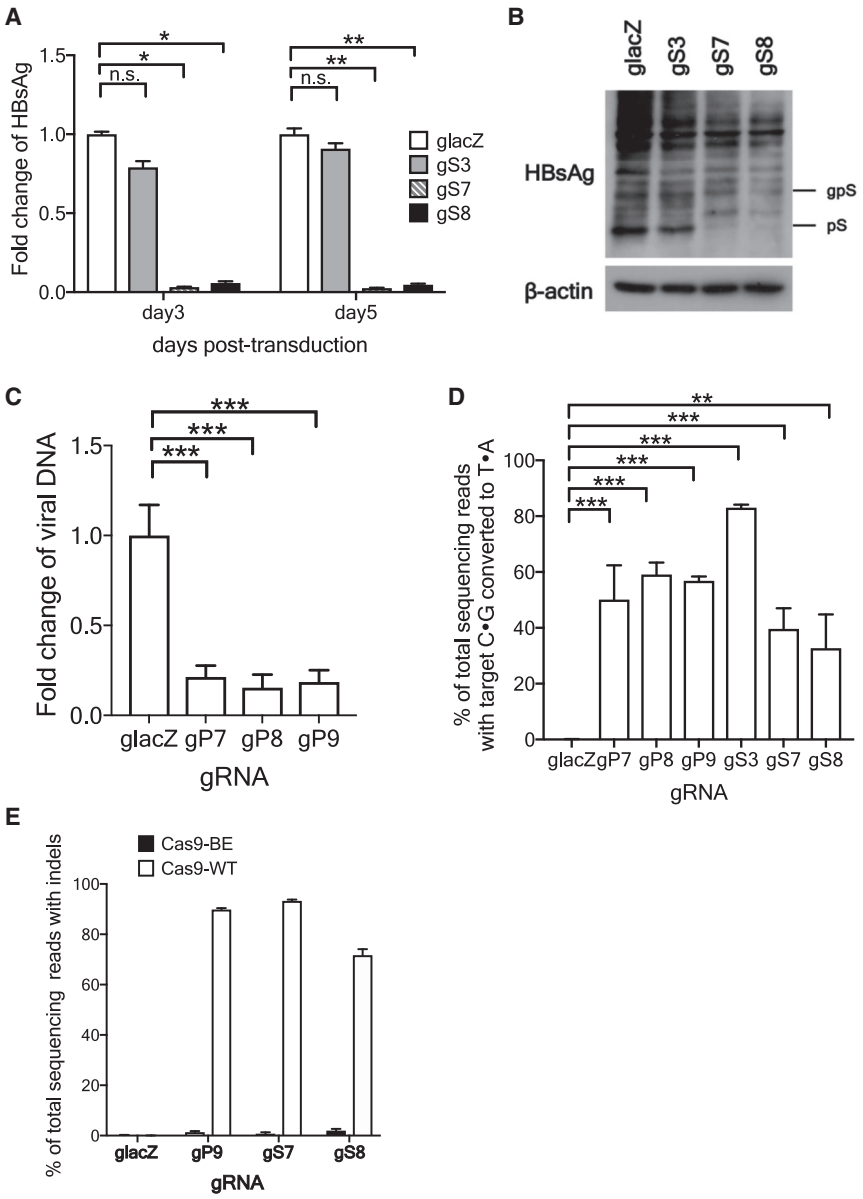

Figure 2. Effect of Base Editing-Introduced Nonsense Mutation on Viral Gene Expression of HepG2.2.15 Cells

(A) Secreted HBsAg levels, measured by the semi-quantitative ELISA assay, in the supernatant of HepG2.2.15 cells transduced with the control gRNA (glacZ) or individual gRNAs gS3, gS7, and gS8 along with the SpCas9 base editor (BE4Gam-P2A-Puro) at day 3 and day 5 post-transduction. The fold change of HBsAg is calculated as the ratio between the indicated HBsAg levels over that of control gRNA (glacZ). (B) Immunoblotting analysis of intracellular HBV surface proteins extracted from the indicated cells of the same experiments in (A). (C) The fold change of supernatant HBV DNA in HepG2.2.15 cells transduced with the glacZ control or the indicated gRNAs gP7, gP8, and gP9. (D) Individual percentages of C-T/G-A conversion at the target sites measured by NGS. (E) Individual percentages of indels compared between Cas9-BE and Cas9-WT at the gRNA-targeting sites measured by NGS. The results of (A) and (C)–(E) are combined from three independent experiments and shown in bar graphs with mean plus standard deviation (SD). *$p < 0.05$, **$p < 0.01$, ***$p < 0.005$ (Student's t test). n.s., not significant.

polymerase mutations W414X-P and G500S (W156X-S) caused a significant reduction of relaxed circular DNA (RC-DNA) to beyond the detection limit (Figure 4E). Taken together, our results confirm that the nucleotide changes at these two particular loci of the HBV genome can result in profound dual suppression of the polymerase and surface gene expression.

Generation of Nonsense Mutations in HBV cccDNA by SpCas9-BE

Since cccDNA is the replicative template of HBV, we further determined whether the SpCas9-BE could indeed generate nonsense mutations in cccDNA, which is an extrachromosomal DNA. We first showed that following HBV infection of HepG2-NTCP-C4 cells *in vitro*, HBV RC-DNA and cccDNA could be detected by Southern blotting (Figure 5A). The identity of cccDNA was further validated by the appearance of 3.2-kb DNA after linearization of RC-DNA and cccDNA with *Eco*RI digestion. Additionally, T5 exonuclease treatment significantly enhanced the purity of cccDNA isolation (Figure 5A). To prove C-T/G-A conversion in cccDNA, we then conducted an experiment by initially repeated transduction of HepG2-NTCP-C4 cells with gRNAs/SpCas9-BE followed by HBV infection. Our preliminary results showed that BE3 exhibited higher base-editing efficacy on cccDNA than did BE4 (data not shown), so we chose BE3 for further experiments. By an immunofluorescence assay (IFA), we showed that the efficiency of HBV infection and delivery of Cas9 was around 22.1% and 15.4%, respectively, and only 4.8% cells were double positive. It is estimated that around 21.7% of HBV-infected cells were positive for Cas9-FLAG (Figure S4). Then we isolated cccDNA from HBV-infected HepG2-NTCP-C4 by T5 exonuclease treatment and analyzed C-T/G-A conversion in cccDNA by Sanger sequencing and NGS (Figures 5B and 5E). The results showed that gP9 and gS8 target sites were effectively edited by SpCas9-BEs at the efficiency close to 50% estimated by Sanger sequencing (Figure 5B). Consistently, the results of NGS analysis showed 25%–35% of base editing (Figure 5E). In addition, BE3 also induced far fewer undesired on-target indels (<0.5%) (Figure 5F). Finally, we demonstrate that the secreted HBsAg levels were significantly decreased in HBV-infected cells treated with gP9 and gS8, and viral DNAs were also significantly

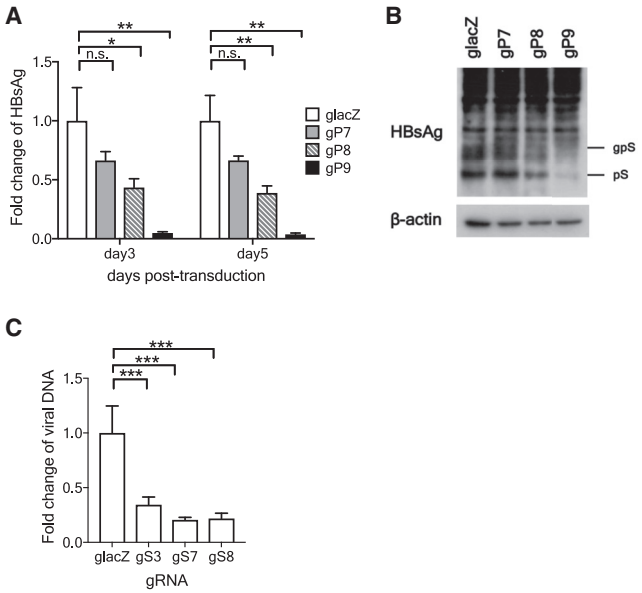

Figure 3. Dual Suppression of HBsAg and Polymerase by SpCas9 Base Editors

(A) The secreted HBsAg levels in the supernatant of HepG2.2.15 cells transduced with SpCas9-BE and individual gRNAs gP7, gP8, gP9, or control glacZ at day 3 and day 5 post-transduction, as the same cells in Figure 2C. (B) Immunoblotting analysis of intracellular HBV surface proteins extracted from the same cells in Figure 2C. (C) The fold change of supernatant HBV DNA in HepG2.2.15 cells treated with the glacZ control or the indicated gRNAs gS3, gS7, and gS8, as the indicated cells of the same experiments in Figure 2A. The results of (A) and (C) are combined from three independent experiments and shown in bar graphs with mean plus standard deviation (SD). *$p < 0.05$, **$p < 0.01$, ***$p < 0.005$ (Student's t test). n.s., not significant.

reduced in cells treated by all these three gRNAs (Figures 5C and 5D). Collectively, our results prove that cccDNA could be base edited to reduce the expression of viral proteins.

DISCUSSION

In this study, we demonstrate that CRISPR/Cas9-mediated BEs could successfully introduce nonsense mutations to specific loci of HBV genomes. The BEs derived from SpCas9 variants VQR, VRER, and EQR were also able to generate nonsense mutations in HBV genomes, further expanding the candidate protospacer sequences. With appropriate gRNAs and BEs, both integrated HBV genomes and cccDNAs could be base edited with high efficacy. More importantly, generation of premature stop codons in the viral surface and polymerase genes of integrated HBV genomes and cccDNAs led to significant reduction of HBsAg secretion and viral replication, a critical step toward HBV cure.

Although Cas9-mediated BEs have been shown to effectively edit a variety of host genomes, their efficacy in episomal forms of viral DNA remains questionable. The core component of the base-editing enzyme is APOBEC, which has been shown to mutate cccDNA.[33] However, little is known about the effects of the subsequent DNA repair mechanisms and the uracil DNA glycosylase inhibitor on the episomal cccDNA. By using the *in vitro* HBV infection system, we proved the nucleotide C to T conversion of cccDNA, which was accompanied by the significant reduction of HBsAg secretion and HBV replication. This is a proof of concept that Cas9-mediated BEs can be utilized to target and silence cccDNA.

Integration of HBV genomes into host chromosomes occurs in the early stage of HBV infection.[7] Although the integrated HBV genome is not a source for productive HBV infection, it often causes continuous secretion of HBsAg, which has long been suggested to suppress the antiviral immunity and allows for establishment of persistent HBV infection. As a result, targeting integrated HBV genomes or silencing surface gene expression to prevent persistent HBsAg secretion is considered a critical step toward the functional cure of HBV.[11,34] Nevertheless, prior attempts to cleave integrated HBV genomes by WT SpCas9 endonuclease may result in host genome large deletions and complex rearrangements, which can cause pathologic consequences.[25] In contrast, Cas9-mediated BEs change the target base in genomic DNA without making DSBs of DNA, and they may reduce the risk of genomic damage. Recently, inactivation of HBV genes by siRNA-based strategies has gained wide interest for silencing the expression of HBsAg, but the effect is transient unless restoration of antiviral immunity can be achieved.[9] Unlike siRNA-based strategies, Cas9-mediated BEs can silence HBV gene expression permanently by introducing nonsense mutations to viral genes. As we show herein, Cas9-mediated BEs effectively generated premature stop codons of the surface gene in both integrated HBV genomes and cccDNAs and reduced HBsAg secretion. Therefore, Cas9-mediated BEs are advantageous for its transient expression to achieve long-term suppression of HBsAg expression, demonstrating its potential for functional HBV cure.

Interestingly, we discovered several HBV genome loci that cause simultaneous nonsense mutation and missense mutation of polymerase and surface genes, respectively, or vice versa, leading to their dual suppression. For example, W414X in the polymerase gene causes G71N in the surface gene, and W156X in the surface gene results in G500S in the polymerase gene. Significant reduction of both polymerase and surface gene expression could be observed when these specific loci of the HBV genome were base edited. G71N (W414X-P) and W156X-S are located in the inner face and the proposed amphipathic helix of surface protein, which are important for S dimer formation.[35,36] The amino acid change of these residues causes the reduction of intracellular and secreted HBsAg, indicating that it may render HBsAg unstable and susceptible to protein degradation. W414X-P and G500S (W156X-S) are located at the palm and finger domains of the polymerase gene, which are critical for viral replication. We further validated the critical role of these residues by generation of W414X in polymerase and W156X in surface genes, respectively, by site-directed mutagenesis. Notably, these two sites and cognate protospacer sequences are highly conserved in 88% and 77% of HBV strains of genotype D (Table S1), so they may serve as ideal targets for a base-editing strategy to treat HBV of genotype D.

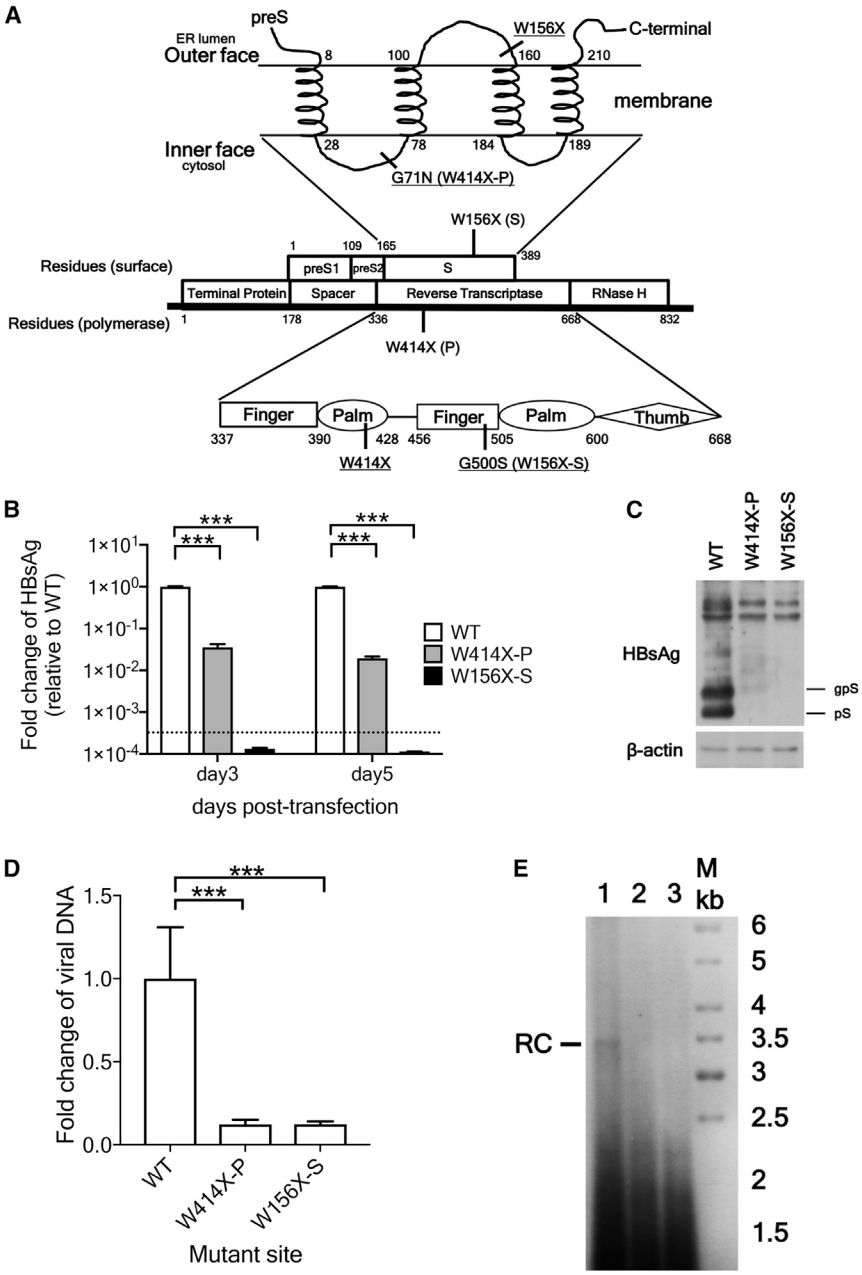

Figure 4. Validation of the Effect of Base-Edited Missense Mutations on the Expression of HBV Surface and Polymerase Proteins

(A) Schematic illustration for the genome organization and protein domains of the HBV surface (S) and polymerase (P) genes, including the overlapping regions of the two genes. The reverse transcriptase domain in P corresponds to part of the S domain in S. The W156X site in S corresponds to G500S in P; the W414X site in P corresponds to G71N in S. (B) The fold change of secreted HBsAg levels in the supernatant of Huh7 cells transfected by 1.3× HBV-WT (WT), 1.3× HBV-W156X in S (W156X-S), or 1.3× HBV-W414X in P (W414X-P) at day 3 and day 5. The dotted line indicates the detection limit of the HBsAg ELISA assay. (C) Immunoblotting analysis of intracellular HBV surface proteins extracted from the indicated cells of the same experiments in (B). (D) Fold change of supernatant HBV DNA in Huh7 cells transfected by the 1.3× HBV-WT (WT), 1.3× HBV-W156X in S (W156X-S), or 1.3 HBV-W414X in P (W414X-P) at day 5. (E) Southern blot analysis of intracellular HBV replicative intermediates in Huh7 cells transfected by WT, W156X-S, or W414X-P 1.3× HBV plasmid, and extracted for genomic DNA by the modified Hirt DNA procedure. The results in (B) and (D) are combined from three independent experiments and shown in bar graphs with means plus standard error (SE). ***$p < 0.005$ (Student's t test). WT, wild-type.

Despite the promising potential of the Cas9-mediated BE as an HBV cure, there remain several daunting challenges, including off-target effects and the difficulty for *in vivo* delivery of Cas9, the same as those faced by WT Cas9 endonuclease.[24] Moreover, mutagenesis with premature stop codons will generate truncated viral proteins and may carry potentially pathogenic or carcinogenic effects, which should be cautiously evaluated. Although we showed that the off-target mutations caused by base editing were quite low, this risk still cannot be ignored.[37] In addition, *in vivo* delivery is particularly challenging for Cas9 BEs because they are larger than WT Cas9 for the appended base-editing domains. Nevertheless, several strategies have been adopted to minimize the off-target effects of Cas9-mediated genome editing.[38,39] Recently, the intein-mediated split-Cas9 systems have also been developed to reduce the insert size to fit the cargo capacity of the AAV system.[40,41] Alternatively, the advance of non-viral delivery systems may improve their *in vivo* delivery efficiency.[42,43] Future study in a disease-relevant animal model is required to prove the *in vivo* efficacy of Cas9 BEs for inactivation of HBV.

In conclusion, Cas9-mediated BEs provide an opportunity for permanent inactivation of both cccDNA and integrated HBV DNA without DSBs of DNA. Combined with NAs, which effectively inhibit ongoing viral replication, Cas9-mediated BEs may eventually achieve the ultimate cure of HBV by suppressing both HBV replication and HBsAg production.

MATERIALS AND METHODS

Plasmids

The human codon-optimized base editing vectors pLenti-FNLS-P2A-Puro (BE3) and pLenti-BE4Gam-P2A-Puro (BE4), as well as U6-gRNA, were obtained from Addgene (Cambridge, MA, USA). The variant VQR (D1135V, R1335Q, and T1337R), VRER (D1135V,

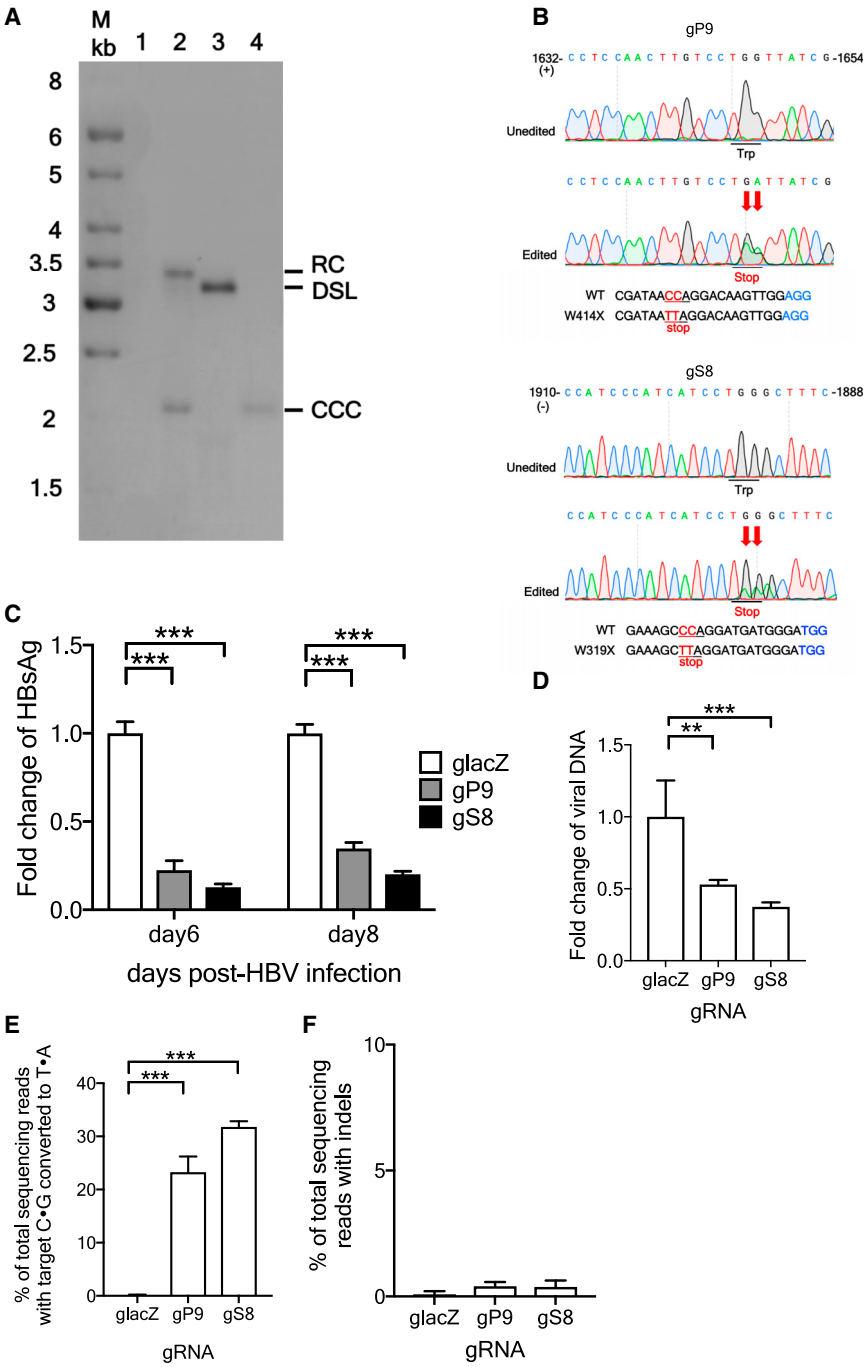

Figure 5. Base Editing of HBV cccDNA

(A) Southern blot analysis of intracellular HBV replicative intermediates of BE/gRNA-transduced HepG2-NTCP-C4 cells infected by 5×10^5 genome equivalents (GEs) of HBV at 9 days post-infection. Lane 1, mock infection; lane 2, HBV infection without enzymatic treatment; lane 3, HBV infection with *Eco*RI treatment; lane 4, HBV infection with T5 exonuclease treatment. RC, HBV RC-DNA; DSL, double-stranded linear DNA; CCC, cccDNA. (B) Sanger sequencing of the base-edited sites in cccDNA targeted by individual gRNAs gP9 and gS8. The labels are the same as those in Figure 1B. (C) The fold change of secreted HBsAg levels, measured by the quantitative HBsAg assay, in the supernatant of HepG2-NTCP-C4 cells at day 6 and day 8 after HBV infection. (D) Fold change of supernatant HBV DNA in HepG2-NTCP-C4 cells transduced by individual gRNAs gP9 and gS8 in comparison to those transduced by the control glacZ. HepG2-NTCP-C4 cells were initially transduced by individual gRNAs, control glacZ, gP9, or gS8, along with SpCas9-BE and subsequently infected by HBV. (E) Individual percentages of C-to-T conversion at the target sites of cccDNA measured by NGS. (F) Individual percentages of indels at the gRNA-targeting sites of cccDNA measured by NGS. The results of (C) and (D)–(F) are combined from three independent experiments and shown in bar graphs with means plus standard error (SE). $^{**}p < 0.01$, $^{***}p < 0.005$ (Student's t test). n.s., not significant.

G1218R, R1335E, and T1337R), EQR (D1135E, R1335Q, and T1337R) were generated by site-directed mutagenesis of the pLenti-BE4Gam-P2A-Puro backbone based on a previous report.[31] The pLenti-U6-gRNA-BSD was generated through Gibson assembly, by combing the U6-BsmBI-sgRNA scaffold and the blasticidin-resistant gene, which was derived from the pLVX.AcGFP.N1 (catalog no. 632154, Clontech) backbone. The resultant gRNAs were subsequently cloned into the plasmid pLenti-U6-gRNA-BSD. The non-vector helper plasmids for lentiviral production, p8.91 and pMD.G, were obtained from the RNAi Core of Academia Sinica, Taiwan. BE-Designer-CRISPR RGEN tools were used to identify the 20-bp protospacer sequences of gRNAs targeting the HBV core, polymerase, surface, and X (http://www.rgenome.net/be-designer/). 1.3× HBV-WT was derived from the pCMV-HBV backbone using Gibson assembly. 1.3× HBV-W156X-S and 1.3× HBV-W414X-P were generated by site-directed mutagenesis of the 1.3× HBV-WT backbone.

Cell Lines and Culture

HEK293T-C, -Pol, and -S cells were generated by transduction of HEK293T cells with lentiviral vector containing the harboring part or the entire ORFs of core, polymerase, and surface genes, respectively, from genotype D HBV. HEK293T, HEK293T-C, HEK293T-Pol, HEK293T-S, HepG2.2.15, and HepAD38 cells were all maintained in Dulbecco's modified Eagle's medium (DMEM, Gibco) supplemented with 10% fetal bovine serum (FBS), 100 U/mL penicillin, and 100 μg/mL streptomycin (Gibco) at 37°C and 5% CO_2. Additionally, 1.5 μg/mL puromycin was added to HEK293T-C, -Pol, and -S. cells, 400 μg/mL G418 was added to HepG2.2.15 cells, and 400 μg/mL G418 and tetracycline were added

to HepAD38 cells. HepG2-NTCP-C4 cells were maintained in DMEM/F12, GlutaMAX (Gibco) containing 10% FBS, 100 U/mL penicillin, and 100 μg/mL streptomycin (Gibco), 5 μg/mL human insulin (ProSpec), 10 mM HEPES (*N*-2-hydroxyethylpiperazine-*N*′-2-ethanesulfonic acid) (Gibco), and 1 mg/mL G418.

Transfection of Cell Lines

DNA transfection was performed using Lipofectamine 3000 according to the manufacturer's protocol with some modifications. For transfection-based editing experiments, HEK293T, HEK293T-C, HEK293T-P, and HEK293T-S cells were seeded to 70%–80% confluence and cotransfected by the expression vectors containing the BE (pLenti-FNLS-P2A-Puro; BE3) and the sgRNA at the ratio of 4:1. For the experiments comparing the viral expression of 1.3× HBV-WT and the derived HBV with site-directed mutagenesis, Huh7 cells were transfected by the indicated plasmids, 1.3× HBV-WT, W414X-P, or W156X-S, and were then harvested at 3 days or 5 days post-transfection. Subsequently, genomic DNAs were extracted by a blood and tissue kit (QIAGEN) and subjected to Sanger sequencing, or Hirt's DNA was extracted for a Southern blotting assay.

Lentiviral Production and Transduction

For the production of lentivirus of BEs pLenti-FNLS-P2A-Puro (BE3) and pLenti-BE4Gam-P2A-Puro (BE4), HEK293T cells were seeded in 10-cm dishes containing 5 μg/mL poly-D-lysine (Sigma, St. Louis, MO, USA). Cells were seeded 1 day before transfection, and, the next day, cells at 95% confluence were transfected with a prepared mix in Opti-MEM (Gibco) containing 6 μg of lentiviral backbone, 4 μg of p8.91, and 2 μg of pMD.G. The media were replaced with Opti-MEM containing 5% FBS, and the culture media were collected after 48 and 72 h. The supernatant was filtered with a 0.4-μm filter (Millipore, Billerica, MA, USA) and subsequently ultracentrifuged with a 20% sucrose cushion in the bottom of the tube and incubated at 26,000 rpm (4°C) for 2 h. The precipitated viral pellet was resuspended in Opti-MEM overnight and then stored at −80°C. For the production of the lentivirus of sgRNAs, HEK293T cells were seeded in a six-well plate containing 5 μg/mL poly-D-lysine (Sigma, St. Louis, MO, USA) 1 day before transfection. On the next day, cells at 95% confluence were transfected with a prepared mix in Opti-MEM containing 1.5 μg of lentiviral backbone, 1 μg of p8.91, and 0.5 μg of pMD.G. The procedures for collection, purification, and storage of lentiviruses are the same as those described above.

Transduction with BE Lentiviruses

For transduction of HepG2.2.15 and HepG2-NTCP-C4 cells, 5×10^5 individual cells were seeded in a 12-well plate. After 24 h, cells were transduced with viral supernatants in the presence of Polybrene (8 μg/μL), and the plates were centrifuged for 1 h at 1,250 × *g*, 32°C. Three days after transduction, cells were treated with puromycin (2.5 μg/mL) and blasticidin S (5 μg/mL) for 7 days of selection. The transduced cells were trypsinized and reseeded at the same number, and subsequently transduced by the same lentivirus again as the above procedures. For the transduced HepG2.2.15 cells, the supernatants were collected at 3 and 5 days after transducing twice with pLenti-BE4Gam-P2A-Puro (BE4), and the cell lysates were collected at 5 days post-transduction. For the HepG2-NTCP-C4 transduction, cells were transduced twice with pLenti-FNLS-P2A-Puro (BE3) and gRNAs.

Preparation and Infection of HBV

Infectious HBV was produced from HepAD38 cells as previously described.[44] The supernatant was harvested and concentrated by 20% sucrose cushion. For the HBV infection experiment, HepG2-NTCP-C4 cells were seeded in a 12-well plate and transduced by pLenti-FNLS-P2A-Puro (BE3) and gRNA lentiviruses. After repeated lentiviral transduction for two times, HBV was infected at 5,000 genome equivalents (GE)/cell. All infections were performed as previously described.[45,46] In addition, HBV was infected into HepG2-NTCP-C4 cells in a 12-well plate at 50,000 GE/cell for cccDNA detection by Southern blot. Briefly, cells were mixed with HBV in the presence of 8% PEG8000 and 5% DMSO at 37°C for 16 h in suspension. To suppress the formation of newly synthesized RC-DNA, infected HepG2-NTCP-C4 cells were treated with 20 μM 3TC (lamivudine) from 3 days after infection.

Sanger and MiSeq Sequencing of Base-Edited Genomic DNA and cccDNA

Genomic DNAs of harvested cells were extracted using a DNase blood and tissue kit (QIAGEN) according to the manufacturer's instructions. The genomic regions of interest were amplified by PCR with the site-specific primers (Table S3) and PfuUltra II fusion HS DNA polymerase (Agilent Technologies) according to the manufacturer's protocol. The PCR products were purified by the Illustra GFX PCR DNA and gel band purification kits (GE Healthcare), and were subjected to Sanger sequencing.

To remove linear and RC-form HBV DNAs for Sanger and MiSeq sequencing of cccDNA, genomic DNAs were extracted and digested with T5 exonuclease (New England Biolabs) in the reaction mixture of 50 μL containing 500 ng of DNA, 5 μL of ,10× reaction buffer and 1 μL of T5 Exo at 37°C for 1 h, and afterward 11 mM EDTA was added to stop reaction.

Immunoblotting Assay

Cells were washed with phosphate-buffered saline (PBS) and lysed with radioimmunoprecipitation assay (RIPA) buffer (50 mM Tris-HCl [pH 7.5], 150 mM NaCl, 1 mM EDTA, 1% Nonidet P-40 [NP-40], 0.5% sodium deoxycholate, 0.1% SDS, protease inhibitor cocktail [Roche]). Whole-cell extracts were subjected to 12% sodium dodecyl sulfate-polyacrylamide gel electrophoresis (SDS-PAGE), followed by western blot analysis using primary antibodies (anti-β-actin [Merck], anti-HBs [Ad/Ay] antibody [ab9193; Abcam, Cambridge, MA, USA]) and secondary antibody and detected by Immobilon Western Chemiluminescent HRP (horseradish peroxidase) substrate (Millipore, Billerica, MA, USA).

ELISA of HBsAg

Elecsys HBsAg II (Roche Diagnostics) was used for HBsAg qualitative determination in the culture supernatant of G2.2.15. Samples with a

signal/cutoff ratio (S/CO) of ≥1 are considered positive, and the values are considered as a semiquantitative level of HBsAg. The quantitative levels of HBsAg in the culture supernatant of HepG2-NTCP-C4 were measured using an Architect HBsAg kit (Abbott Laboratories). The calibration range recommended by the manufacturer was from 0 to 250 IU/mL. The positivity criterion of HBsAg was ≥0.05 IU/mL.

Quantitative Real-Time PCR

The viral DNAs were purified from the supernatant of G2.2.15 using a DNase blood and tissue kit (QIAGEN) according to the manufacturer's instructions. The PCR reaction was performed in a total volume of 10 μL, which contains 4 μL of DNA template, 0.25 μM for each primer, a 0.1 μM probe, and 5 μL of TaqMan master mix. The program was 2 min at 50°C, 10 min at 95°C, and 40 cycles of 95°C for 15 s and 60°C for 1 min. The probe and primer sequences are listed in Table S3.

HBV DNA Extraction and Southern Blotting

HBV DNA was extracted by the modified Hirt method as previously described.[18] Infected HepG2-NTCP-C4 was lysed in Hirt's buffer (0.7% SDS, 10 mM Tris-HCl [pH 8.0], and 10 mM EDTA [pH 8.0]). The lysates were treated with 5 M NaCl and incubated at 4°C overnight and then centrifuged at 10,000 rpm for 30 min at 4°C. For extraction of DNA, the supernatant was treated by saturated phenol twice and phenol/chloroform (1:1) once. DNA was precipitated with 2× vol of 100% ethanol at room temperature overnight and subsequently precipitated at 10,000 rpm centrifugation at 4°C for 30 min. 30 μg of Hirt DNA was analyzed by the modified Southern blot method as previously described.[18]

DNA Library Preparation and MiSeq Sequencing

A Thermo Scientific Phusion high-fidelity DNA polymerases kit was used according to the manufacturer's recommendations (Illumina) for DNA library preparation. Adaptor-ligated DNA was indexed and enriched through limited-cycle PCR. The DNA library was quantified with NanoDrop and through real-time PCR. The DNA library was loaded on an Illumina MiSeq instrument according to the manufacturer's instructions and sequenced with 600 cycles by the Medical Microbiota Center of the First Core Laboratory, National Taiwan University College of Medicine.

The quality of raw reads was evaluated by FastQC. Base editing efficiency and indel rates of each sample were calculated using a Python script. Briefly, the sequence of gRNA target regions in each read was identified by splitting the reads by 10-bp flanking sequences with exact matches on both sides of the target regions. Indels were calculated as the number of reads with target regions that contain insertions or deletions divided by the total read number. Base editing efficiency was measured by counting the number of A, T, C, and G bases at each position on the target sequences and then the numbers were divided by the number of total reads. The ratios of induced premature stop codons in each sample were determined by dividing the number of reads containing induced premature stop codons with the number of total reads.

Statistical Analysis

An unpaired, two-sided Student's t test was used to compare the difference between two independent groups. Data associated with this study are present in the text or in Supplemental Materials and Methods.

SUPPLEMENTAL INFORMATION

Supplemental Information can be found online at https://doi.org/10.1016/j.omtn.2020.03.005.

AUTHOR CONTRIBUTIONS

Conceptualization and Methodology, Y.-C.Y., Y.-H.C., and H.-C.Y.; Investigation, Y.-C.Y., C.C., C.-C.W., C.-H.T., I.-J.L., and F.-Y.W; Software, Y.-H.C.; Writing – Original Draft & Review & Editing, Y.-C.Y. and H.-C.Y.; Supervision, H.-C.Y., J.-H.K., P.-J.C., D.-S.C., and C.-J.L.

CONFLICTS OF INTEREST

The authors declare no competing interests.

ACKNOWLEDGMENTS

We thank Lukas Dow and George Church for donating plasmids (pLenti-FNLS-P2A-Puro, pLenti-BE4Gam-P2A-Puro, and U6-gRNA) to Addgene. We thank Dr. Mei-Ru Chen and Yu-Ching Dai for assistance with cell confocal imaging analysis. We are also grateful for Dr. Yu-Chi Chou and Dr. Cheng-Pu Sun at the Academia Sinica for much useful input and valuable comments on this manuscript. We would like to acknowledge the MiSeq and sequencing service provided by the Medical Microbiota Center of the First Core Laboratory, National Taiwan University College of Medicine, and the Department of Medical Research, National Taiwan University Hospital. This work was supported by grants from the National Taiwan University Hospital (NTUH, 108-s4135), MOST (104-2314-B-002-041-MY3), and the Cardinal Tien Junior College of Healthcare and Management (CTCN-107-04).

REFERENCES

1. Yang, H.C., and Kao, J.H. (2016). Revisiting the natural history of chronic HBV infection. Curr. Hepatol. Rep. *15*, 141–149.

2. Papatheodoridis, G., Vlachogiannakos, I., Cholongitas, E., Wursthorn, K., Thomadakis, C., Touloumi, G., and Petersen, J. (2016). Discontinuation of oral antivirals in chronic hepatitis B: A systematic review. Hepatology *63*, 1481–1492.

3. Nassal, M. (2015). HBV cccDNA: viral persistence reservoir and key obstacle for a cure of chronic hepatitis B. Gut *64*, 1972–1984.

4. Lok, A.S., Zoulim, F., Dusheiko, G., and Ghany, M.G. (2017). Hepatitis B cure: from discovery to regulatory approval. Hepatology *66*, 1296–1313.

5. Revill, P.A., Chisari, F.V., Block, J.M., Dandri, M., Gehring, A.J., Guo, H., Hu, J., Kramvis, A., Lampertico, P., Janssen, H.L.A., et al.; Members of the ICE-HBV Working Groups; ICE-HBV Stakeholders Group Chairs; ICE-HBV Senior Advisors (2019). A global scientific strategy to cure hepatitis B. Lancet Gastroenterol. Hepatol. *4*, 545–558.

6. Mason, W.S., Gill, U.S., Litwin, S., Zhou, Y., Peri, S., Pop, O., Hong, M.L., Naik, S., Quaglia, A., Bertoletti, A., et al. (2016). HBV DNA integration and clonal hepatocyte expansion in chronic hepatitis B patients considered immune tolerant. Gastroenterology *151*, 986–998.e4.

7. Tu, T., Budzinska, M.A., Shackel, N.A., and Urban, S. (2017). HBV DNA integration: molecular mechanisms and clinical implications. Viruses *9*, E75.
8. Seeger, C., and Mason, W.S. (2015). Molecular biology of hepatitis B virus infection. Virology *479-480*, 672–686.
9. Wooddell, C.I., Yuen, M.F., Chan, H.L., Gish, R.G., Locarnini, S.A., Chavez, D., Ferrari, C., Given, B.D., Hamilton, J., Kanner, S.B., et al. (2017). RNAi-based treatment of chronically infected patients and chimpanzees reveals that integrated hepatitis B virus DNA is a source of HBsAg. Sci. Transl. Med. *9*, eaan0241.
10. Bertoletti, A., and Ferrari, C. (2016). Adaptive immunity in HBV infection. J. Hepatol. *64* (1, Suppl), S71–S83.
11. Cornberg, M., and Manns, M.P. (2018). Hepatitis: no cure for hepatitis B and D without targeting integrated viral DNA? Nat. Rev. Gastroenterol. Hepatol. *15*, 195–196.
12. Stone, D., Niyonzima, N., and Jerome, K.R. (2016). Genome editing and the next generation of antiviral therapy. Hum. Genet. *135*, 1071–1082.
13. Kennedy, E.M., and Cullen, B.R. (2017). Gene editing: a new tool for viral disease. Annu. Rev. Med. *68*, 401–411.
14. Bloom, K., Ely, A., Mussolino, C., Cathomen, T., and Arbuthnot, P. (2013). Inactivation of hepatitis B virus replication in cultured cells and *in vivo* with engineered transcription activator-like effector nucleases. Mol. Ther. *21*, 1889–1897.
15. Chen, J., Zhang, W., Lin, J., Wang, F., Wu, M., Chen, C., Zheng, Y., Peng, X., Li, J., and Yuan, Z. (2014). An efficient antiviral strategy for targeting hepatitis B virus genome using transcription activator-like effector nucleases. Mol. Ther. *22*, 303–311.
16. Jinek, M., Chylinski, K., Fonfara, I., Hauer, M., Doudna, J.A., and Charpentier, E. (2012). A programmable dual-RNA-guided DNA endonuclease in adaptive bacterial immunity. Science *337*, 816–821.
17. Jiang, W., and Marraffini, L.A. (2015). CRISPR-Cas: new tools for genetic manipulations from bacterial immunity systems. Annu. Rev. Microbiol. *69*, 209–228.
18. Lin, S.R., Yang, H.C., Kuo, Y.T., Liu, C.J., Yang, T.Y., Sung, K.C., et al. (2014). The CRISPR/Cas9 system facilitates clearance of the intrahepatic HBV templates *in vivo*. Mol. Ther. Nucleic Acids *3*, e186.
19. Seeger, C., and Sohn, J.A. (2014). Targeting hepatitis B virus with CRISPR/Cas9. Mol. Ther. Nucleic Acids *3*, e216.
20. Karimova, M., Beschorner, N., Dammermann, W., Chemnitz, J., Indenbirken, D., Bockmann, J.H., Grundhoff, A., Lüth, S., Buchholz, F., Schulze zur Wiesch, J., and Hauber, J. (2015). CRISPR/Cas9 nickase-mediated disruption of hepatitis B virus open reading frame S and X. Sci. Rep. *5*, 13734.
21. Liu, X., Hao, R., Chen, S., Guo, D., and Chen, Y. (2015). Inhibition of hepatitis B virus by the CRISPR/Cas9 system via targeting the conserved regions of the viral genome. J. Gen. Virol. *96*, 2252–2261.
22. Ramanan, V., Shlomai, A., Cox, D.B., Schwartz, R.E., Michailidis, E., Bhatta, A., Scott, D.A., Zhang, F., Rice, C.M., and Bhatia, S.N. (2015). CRISPR/Cas9 cleavage of viral DNA efficiently suppresses hepatitis B virus. Sci. Rep. *5*, 10833.
23. Ely, A., Moyo, B., and Arbuthnot, P. (2016). Progress with developing use of gene editing to cure chronic infection with hepatitis B virus. Mol. Ther. *24*, 671–677.
24. Yang, H.C., and Chen, P.J. (2018). The potential and challenges of CRISPR-Cas in eradication of hepatitis B virus covalently closed circular DNA. Virus Res. *244*, 304–310.
25. Kosicki, M., Tomberg, K., and Bradley, A. (2018). Repair of double-strand breaks induced by CRISPR-Cas9 leads to large deletions and complex rearrangements. Nat. Biotechnol. *36*, 765–771.
26. Rees, H.A., and Liu, D.R. (2018). Base editing: precision chemistry on the genome and transcriptome of living cells. Nat. Rev. Genet. *19*, 770–788.
27. Komor, A.C., Kim, Y.B., Packer, M.S., Zuris, J.A., and Liu, D.R. (2016). Programmable editing of a target base in genomic DNA without double-stranded DNA cleavage. Nature *533*, 420–424.
28. Schatoff, E.M., Zafra, M.P., and Dow, L.E. (2019). Base editing the mammalian genome. Methods *164–165*, 100–108.
29. Komor, A.C., Zhao, K.T., Packer, M.S., Gaudelli, N.M., Waterbury, A.L., Koblan, L.W., Kim, Y.B., Badran, A.H., and Liu, D.R. (2017). Improved base excision repair inhibition and bacteriophage Mu Gam protein yields C:G-to-T:A base editors with higher efficiency and product purity. Sci. Adv. *3*, eaao4774.
30. Zafra, M.P., Schatoff, E.M., Katti, A., Foronda, M., Breinig, M., Schweitzer, A.Y., Simon, A., Han, T., Goswami, S., Montgomery, E., et al. (2018). Optimized base editors enable efficient editing in cells, organoids and mice. Nat. Biotechnol. *36*, 888–893.
31. Kleinstiver, B.P., Prew, M.S., Tsai, S.Q., Topkar, V.V., Nguyen, N.T., Zheng, Z., Gonzales, A.P., Li, Z., Peterson, R.T., Yeh, J.R., et al. (2015). Engineered CRISPR-Cas9 nucleases with altered PAM specificities. Nature *523*, 481–485.
32. Sells, M.A., Chen, M.-L., and Acs, G. (1987). Production of hepatitis B virus particles in Hep G2 cells transfected with cloned hepatitis B virus DNA. Proc. Natl. Acad. Sci. USA *84*, 1005–1009.
33. Lucifora, J., Xia, Y., Reisinger, F., Zhang, K., Stadler, D., Cheng, X., Sprinzl, M.F., Koppensteiner, H., Makowska, Z., Volz, T., et al. (2014). Specific and nonhepatotoxic degradation of nuclear hepatitis B virus cccDNA. Science *343*, 1221–1228.
34. Zoulim, F. (2018). Inhibition of hepatitis B virus gene expression: a step towards functional cure. J. Hepatol. *68*, 386–388.
35. Stirk, H.J., Thornton, J.M., and Howard, C.R. (1992). A topological model for hepatitis B surface antigen. Intervirology *33*, 148–158.
36. Suffner, S., Gerstenberg, N., Patra, M., Ruibal, P., Orabi, A., Schindler, M., and Bruss, V. (2018). Domains of the hepatitis B virus small surface protein S mediating oligomerization. J. Virol. *92*, e02232-17.
37. Zuo, E., Sun, Y., Wei, W., Yuan, T., Ying, W., Sun, H., Yuan, L., Steinmetz, L.M., Li, Y., and Yang, H. (2019). Cytosine base editor generates substantial off-target single-nucleotide variants in mouse embryos. Science *364*, 289–292.
38. Kim, D., Luk, K., Wolfe, S.A., and Kim, J.S. (2019). Evaluating and enhancing target specificity of gene-editing nucleases and deaminases. Annu. Rev. Biochem. *88*, 191–220.
39. Zhou, C., Sun, Y., Yan, R., Liu, Y., Zuo, E., Gu, C., Han, L., Wei, Y., Hu, X., Zeng, R., et al. (2019). Off-target RNA mutation induced by DNA base editing and its elimination by mutagenesis. Nature *571*, 275–278.
40. Truong, D.J., Kühner, K., Kühn, R., Werfel, S., Engelhardt, S., Wurst, W., and Ortiz, O. (2015). Development of an intein-mediated split-Cas9 system for gene therapy. Nucleic Acids Res. *43*, 6450–6458.
41. Zetsche, B., Volz, S.E., and Zhang, F. (2015). A split-Cas9 architecture for inducible genome editing and transcription modulation. Nat. Biotechnol. *33*, 139–142.
42. Yin, H., Kanasty, R.L., Eltoukhy, A.A., Vegas, A.J., Dorkin, J.R., and Anderson, D.G. (2014). Non-viral vectors for gene-based therapy. Nat. Rev. Genet. *15*, 541–555.
43. Li, L., Hu, S., and Chen, X. (2018). Non-viral delivery systems for CRISPR/Cas9-based genome editing: challenges and opportunities. Biomaterials *171*, 207–218.
44. Ladner, S.K., Otto, M.J., Barker, C.S., Zaifert, K., Wang, G.H., Guo, J.T., Seeger, C., and King, R.W. (1997). Inducible expression of human hepatitis B virus (HBV) in stably transfected hepatoblastoma cells: a novel system for screening potential inhibitors of HBV replication. Antimicrob. Agents Chemother. *41*, 1715–1720.
45. Yan, H., Zhong, G., Xu, G., He, W., Jing, Z., Gao, Z., Huang, Y., Qi, Y., Peng, B., Wang, H., et al. (2012). Sodium taurocholate cotransporting polypeptide is a functional receptor for human hepatitis B and D virus. eLife *1*, e00049.
46. Iwamoto, M., Watashi, K., Tsukuda, S., Aly, H.H., Fukasawa, M., Fujimoto, A., Suzuki, R., Aizaki, H., Ito, T., Koiwai, O., et al. (2014). Evaluation and identification of hepatitis B virus entry inhibitors using HepG2 cells overexpressing a membrane transporter NTCP. Biochem. Biophys. Res. Commun. *443*, 808–813.